ANALYSIS OF SPECTRAL AND PHOTOMETRIC OBSERVATIONS OF THE CH CYG SYMBIOTIC STAR IN 2018

Kh. M. Mikailov [a], ***R. T. Mammadov*** [b], ***A. J. Orujova*** [a], ***O. V. Khalilov*** [a], ***I. A. Alekberov*** [a*]

[a] *Shamakhy Astrophysical Observatory named after N.Tusi, Azerbaijan National Academy of Sciences, Shamakhy region, Azerbaijan*

[b] *Batabat Astrophysical Observatory of Nakhchivan branch of ANAS*

The paper presents the results of a comparative analysis of the star's light curve with the spectrophotometric parameters of the Hα, Hβ, NaI doublets lines of the D1, D2 and HeI 5876 measured on the basis of highly resolved echelle spectra of the symbiotic star CH Cyg obtained in the 2018^{th} ShAO telescope in 2018 using a modern light receiver. The results of the analysis showed that the equivalent width and intensity of the Hα, Hβ and HeI 5876 emission lines increase with decreasing star brightness. Even at maximum brightness, the HeI 5876 line disappears. Changes in the values of equivalent widths and intensities of the components of the Hβ line and the light curve V show the same character with the opposite phase. High-velocity wide absorption components with a speed of up to 800 km/s were found in the Hβ and HeI 5876 lines.
The NaI doublet absorption line proles show a two-component structure, and the change in depth $(1 - I/I_0)$ of the red components of the D1 and D2 lines indicates exactly the same feature as the brightness change V.

Keywords: Symbiotic star – CH Cyg – echelle spectra – V magnitude – line profile – equivalent width.

1. INTRODUCTION

CH Cyg is very complex and mysterious variable comprehensively studied in a very large spectralscale. CH Cyg is symbiotic star was revealed in 80^{th} years of 19^{th} century. Photometric observation history for more than 130 years period is available for thisstar [12]. This is the brightest the closestone among symbiotics.

* E-mail: mikailov.kh@gmail.com

The distanceto this symbioticstaris about 244 pc accordingto data of Hipparcos [15].

Its visual magnetude is $V = 6.0^m$ min maximumand 10.5^m in minimum, it is brighte in infrared ray and magnetude in 2μm is $K = -1^m$. First useful spectra of CH Cyg have been achieved by Joy in 1924 and 1927 [9]. According to 100 days period of well disseminated 5 spectra the spectral type of the star has been determined M6 and radial velocity has been determined -52.5 km/s. There is no information available about emission lines. In 1952 Gaposhkin classifed [5] the CH Cyg as M6-M7 spectral class varying in 90-100 days period in 1^m amplitude by analyzing the Harvard patrol observation materials. It was even accepted as a standard star because these alterations were non noticeable in the spectrum. This classifcation was accepted true until 1963. For the first time Deutsch revealed a strong alteration in the spectrum of the star on September 1963 [4]. In the spectrumof the star hot blue continuum and emission lines of HI, HeI, [FeII] CaII were observed along with absorption lines of neutral metal, which is the sign of a cold star. It repeated in 1965 again. Since that time the star attracted attentions and was accepted as a symbiotic star.

Periodic photometric, infrared, spectral and radio observations have been conducted thanks to convenient location of the star-in the north hemisphere at $+50°$.

Observations show that repetitive active processes occur in the star in various periods. Composition of the star has not been fully identifed yet:binaryand triple star system models havebeen proposed [6].

Nowadays, CH Cyg is one of the most researched and the least understood objects [3]. It is accepted that the activness of CH Cyg this star is generated from the energy released as a result of accretion of the red giant'swind by the hot component. The amount of accreting substance is dependent on pulsation of the giant and also on orbital movement of the star, of course if the orbit is elliptic. Several possible commonly accepted models have been proposed to explain the CH Cyg symbiotic system.

Magneticrotator model [12], according to this model the CH Cyg is a binary star system comprising of a pulsating red giant and white dwarf with a powerful magnetic feld mowing in 5700 days period in an elliptic orbit. Hinkle [6] identifed 756^d period of periodic of radial velocity in the spectr of CH Cyg. They explainedit with existence of the third G-dwarf in the inner orbit with a short period ($P = 756^d$) within the long period ($P = 5300^d$) of binary system. Later, after several observations and precisions, Hinkle refused from the triple stars model and proposed binary symbiotic system for the CH Cyg [7].

By proposing a long period 5650^d in [10] 1998-2001 Mikailov, based on spectra achieved in 1995-2004 Ijima et al. identifed that 756^d period in radial velocity existsin opticregion too for the spectrum lines of thered giant.

Table 1. Log of Spectral observations of CH Cyg in 2018

Spectrum number in the catalogue	Observation	UT date (day.month.year)	JD2458000+	Exp(s)	number of spectra
KF2271-72.fit	03.05.2018	21:27:03	242.39378	1500	2
KF2288-89.fit	05.05.2018	19:58:46	244.33248	1800	2
KF2431-32-33.fit	24.05.2018	21:26:14	263.39322	1500	3
KF2454.fit	04.06.2018	21:07:22	274.38012	1500	1
KF2483.fit	16.06.2018	21:51:45	286.41094	1200	1
KF2497-98-99.fit	19.06.2018	17:56:55	289.24786	1200	3
KF2508-09-10.fit	21.06.2018	18:42:22	291.27942	1500	3
KF2524-25-26.fit	22.06.2018	17:59:38	292.24975	1500	3
KF2533-39.fit	23.06.2018	19:43:00	293.32153	1500	7
KF2569-70.fit	25.06.2018	19:45:17	295.32311	1500	2
KF2580-81.fit	25.06.2018	21:24:36	295.39208	1500	2
KF2622-26.fit	26.06.2018	21:40:00	296.40278	1500	3
KF2666-67-84-85-92.fit	28.06.2018	23:36:59	298.48402	1500	5
KF2695-98.fit	29.06.2018	18:27:48	299.26931	1500	4
KF2709-11.fit	29.06.2018	20:02:43	299.33522	1500	3
KF2722-25.fit	30.06.2018	18:32:42	300.27271	1500	4
KF2753-56.fit	01.07.2018	18:28:46	301.26998	1500	4
KF2794-95.fit	02.07.2018	17:39:50	302.235995	1500	2
KF2812-13.fit	02.07.2018	19:57:49	302.331817	1500	2
KF2856-57.fit	05.07.2018	19:40:18	305.319653	1500	2
KF2916-17-26.fit	18.07.2018	19:32:48	318.314444	1500	3
KF2940-41.fit	19.07.2018	17:25:09	319.225799	1500	2
KF2942-43.fit	19.07.2018	18:16:07	319.261192	1500	2
KF2975-76.fit	24.07.2018	17:24:16	324.225185	1500	2
KF3011-12-13.fit	26.07.2018	17:55:05	326.246586	1500	3
KF3063-64.fit	29.07.2018	19:06:04	329.29588	1500	2
KF3071-72.fit	30.07.2018	17:28:16	330.227963	1500	2
KF3096-97.fit	02.08.2018	17:25:43	333.226192	1500	2
KF3149.fit	08.08.2018	19:54:23	339.329433	1500	1
KF3166-67.fit	16.08.2018	16:56:25	347.205845	1500	2
KF3273-76.fit	26.08.2018	19:58:53	357.332558	1500	4
KF3319-22.fit	29.08.2018	21:53:59	360.412488	1500	4
KF3325-28.fit	30.08.2018	0:00:23	359.500266	1500	4
KF3357-58.fit	30.08.2018	21:07:24	361.380139	1500	2
KF3361-62.fit	30.08.2018	22:41:33	361.445521	1500	2
KF3373-74.fit	11.12.2018	15:08:20	464.130787	2000	2
KF3382-83.fit	12.12.2018	15:41:12	465.153611	1800	2

These results confrmed that CH Cyg symbiotic system consists of 3 stars.

We CH Cyg symbiotic star introduce the comparison of the spectral parameters of Hα, Hβ, HeI 5876 and NaI doublet lines V light curve of the star based on spectra achieved on Shamakhy Observatory in 2018.

2. OBSERVATIONS AND DATA REDUCTION

All echelle spectra discussed in this paper have been managed in 2 meters telescope of Shamakhy Astrophysical Observatory in 2018 between May÷December, during 31 nights.The telescope is fitted with ShAFES - Shamakhy Fibre Echelle Spectrograph and CCD camera cooled by liquid nitrogen (Mikailov Kh.et al.2020).

Spectral identifcation R=$\lambda/\Delta\lambda$=28000, spectral diapason 3900-7700 Å, chip 4096×4096 pixel, pixel size 15×15μm. All spectra have been achieved in SLW regime of CCD, gain=1.27 e-/ADU, Read Out Noise (RON) =3.74.

All calibration screens have been achieved for each night: Sky, ThAr, Flat and Darks.

The interval of the observation period was 223 days and in this period nearly 100 echelle spectrum have been achieved. All spectra have been achieved within 119 days in sequence, just 2 spectr have been achieved after about ∼100 days.

Spectra of the stars a Lyr and 51 Dracon have been achieved in the same conditions for processing of the telluric lines in the spectra of CH Cyg symbiotic star and spectra of HD148783 (G Her, M6III) have been achieved in some nights for processing of the cold star M spectra.Wavelength calibration achieved with Sky and a ThAr hollow cathode comparison. The spectra were reduced using the software package new version of DECH (www.gazinur.com/DECH-software.htm)following the standard procedures. Extraction of all spectra have been managed by using IRAF mask.

Observation history is given in the table 1.Catalogue list of the spectra and date of achievement, universal time, exposition time and number of spectra achieved within a night have been given in the table.

3. PHOTOMETRICS OF CH CYG

17 nights of photometric observations of CH Cyg have been carried out in ZEISS-600 telescope of Shamakhy Astrophysics Observatory in 2018 July September. The telescope was fitted with 4096×4096 pixel (1 pix = 9 mic) size CCD type of light receiver and photometer with efective fields of view are of 17 arcmin (Abdullayev et al. 2012).

Light curve in V filter for the period of spectral observations of CH Cyg symbiotic star was composed based on our observations and AAVSO7 (www.aavso.org/lcg) database (Fig. 1). In the figure 1 empty circles match with the dates of observations. As it is seen from the figure, the star as active during observations and with in several days it got weakened by 1.5^m and reduced from 6.5^m to 8^m. It got its previous brightness after about 1 month. Fortunately, our spectral observations coincided with that period and covered that dramatic phase of the star.

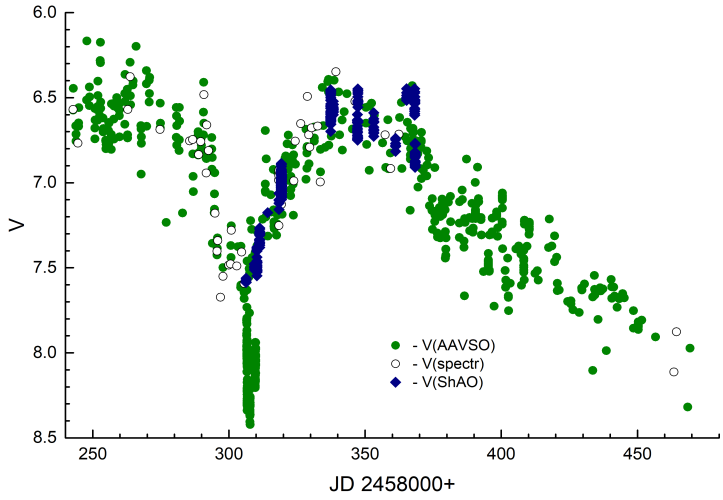

Fig. 1. Light curve of the CH Cyg symbiotic star in V filter. •- AAVSO,▲- ShAO data, ○- dates of spectral observations.

4. RESULTS OF MEASUREMENTS

In this paper we only worked with Hα and Hβ lines of Balmer series of the Hydrogen atom, HeI 5876 line of Helium atom, doublet lines of NaI D1 and D2 lines of Natrium atom. In the next studies it is planned to researches with the other spectral lines. Hα and Hβ lines are very bright and intense as radiation lines, hence it is possible to identify the structure of their profiles with high definition.

5. Hα AND Hβ HYDROGEN LINES

Profiles of Hα and Hβ lines are given in the Fig. 2. As it is seen from the figure,Hα and Hβ lines gave profiles with intensive alteration, centric absorption

and with binary V (Violet) and R (Red) components during period of observations.

In all the spectra red component was more intensive than blue component, e.g.:8V/R<1. It indicates that all time through observations continuous flow of substance occurred. In some profiles the central absorption reduces, even lower than continuum. Large absorption components with high speed have been observed in the violet side of Hβ line. Speed in the violet side of absorption components varies between -660 ÷ -900 km/s. Spectral parameters (ray speed, intensity,

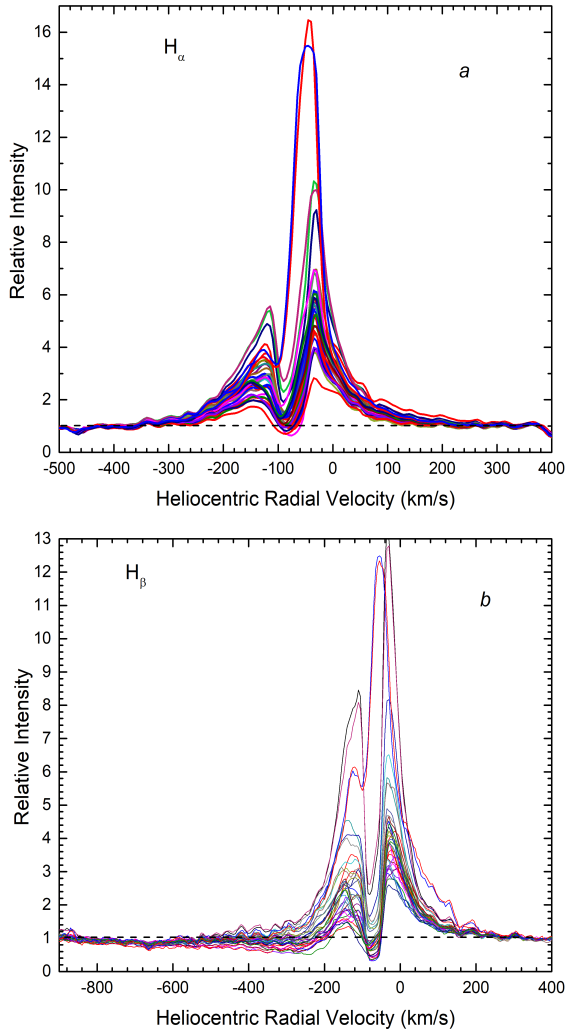

Fig. 2. Profiles of Hydrogen lines. a – Hα line, b – Hβ line. Continuum is indicated with dash line.

equivalent widths) of Hα and Hβ have been given in the table 2 and 3. Ray speed of R component of Hα line was almost in close value in all the dates: RV= -31÷-33 km/s. Only in the last two dates - 11^{th} and 12^{th} of December it slides towards 9 to the violet side in about in 10 km/s and was RV= -43,÷-45 km/s. Ray speed of V component was changed in -116 ÷ -130 km/s, and central absorption was changed in -75 ÷ -103 km/s. Alterations in ray speed is perhaps connected with alterations of intensity of V and R components. Ray speed of the second component of the V component is measured -145 ÷ -150 km/s. As it is seen from the table 2, intensity and equivalent width of components of Hα line changes in about -5 times during the period of observations. Intensity of R component gets values in 2.8 ÷ 16.4 interval, and intensity of V component is gets values in 1.73 ÷ 5.56 interval.

While measuring the equivalent width of Hα and Hβ components the deepest point of the central absorption was taken as a border. That's why values of equivalent width of components should be considered as conditional. Equivalent width in Hα lines got values in the 4.81 ÷ 29.2 Åinterval. The minimum value was recorded in 26-08-2018 and in that date HeI line disappeared.

Hβ line's R component's ray speed alters more than Hα during observation period: RV= -7.4÷-33 km/s, and it got RV= -52÷-54 km/s by sliding towards to the violet side on 11^{th} and 12^{th} of December by ∼30 km/s. Most probably alteration in the speed is due to sharp change in intensity of R component. Ray speed of the Hβ line R component was -104 ÷ -153 km/s, and ray speed of the central adsorption was close to Hα: -70 ÷ -100 km/s. Alteration of ray speed perhaps is due to changes in intensity of R and V components.

As it is seen from table 3, intensity and equivalent changes rapidly at the same observation period. Intensity of R component gets value of 2.2 ÷ 12.84 and intensity of V component gets value of 1.63 ÷ 8.47. Increasement of intensity of V component was 1.7 times more in Hβ line than in Hα line. Equivalent width of Hβ line got value in 3.05 ÷ 23.94 Å. Minimum and maximum proportion of values of equivalent widths of Hα and Hβ line were 6 and 8 respectively.

6. HEI 5876 AND NAI DOUBLET LINES

HeI λ 5876 and NaI doublet lines are the most visible lines after Balmer series lines of Hydrogen in the CH Cyg symbiotic star spectrum. HeI λ 5876 is generated in the adjacent cover around the hot star in the star wind. NaI doublet lines are indicators of star surrounding cover and neutral material zone. Study of these lines will allow to characterize the afore mentioned environments. HeI 5876 and NaI doublet lines profiles are given in the Fig.3. As it is clear from the figure, HeI 5876 and NaI doublet lines changed rapidly during observation season. In parallel

Table 2. Results of measurements of parameters of Hα line.

JD 2458000+	RVkm/s				İnt		EW(Å)		
	R	MU	V1	V2	R	V	R	V	R+V
242.3938	-30.90	-75.40	-124.00		5.70	3.90	9.20	6.25	15.45
244.3325	-30.60	-78.50	-124.00		5.85	4.20	10.45	6.39	16.85
263.3932	-32.40	-77.50	-127.00		5.34	3.68	6.88	6.15	13.03
274.3800	-31.79	-77.64	-125.90		3.98	2.30	6.40	3.52	10.07
286.4109	-31.98	-83.26	-128.28		4.92	2.95	6.86	4.48	11.35
289.2479	-31.90	-89.90	-129.40		9.26	4.85	13.27	7.63	20.09
291.2791	-32.24	-81.74	-127.46		5.58	2.95	7.47	4.39	11.86
292.2497	-32.34	-83.85	-123.64		5.67	3.34	7.80	4.95	12.76
293.2864	-32.44	-81.74	-127.46		6.05	3.60	7.80	4.91	12.72
295.3231	-32.92	-84.46	-125.10		5.40	3.50	6.77	5.27	12.04
295.3921	-32.65	-84.89	-125.44		5.24	2.96	6.90	4.45	11.34
296.4028	-34.00	-86.65	-123.02		5.59	3.37	7.28	5.33	12.61
298.4840	-31.85	-84.08	-122.77		6.95	3.19	9.02	5.21	14.23
299.2693	-32.69	-87.82	-117.61		10.25	5.42	14.48	8.75	23.24
299.3352	-32.97	-88.78	-116.39		9.96	5.56	15.45	9.08	24.51
300.2727	-33.53	-84.72	-124.78		6.08	2.76	7.25	4.29	11.54
301.2700	-33.12	-86.26	-123.80		6.10	2.81	7.51	4.50	12.02
295.3231	-32.92	-84.46	-125.10		5.40	3.50	6.77	5.27	12.04
295.3921	-32.65	-84.89	-125.44		5.24	2.96	6.90	4.45	11.34
296.4028	-34.00	-86.65	-123.02		5.59	3.37	7.28	5.33	12.61
298.4840	-31.85	-84.08	-122.77		6.95	3.19	9.02	5.21	14.23
299.2693	-32.69	-87.82	-117.61		10.25	5.42	14.48	8.75	23.24
299.3352	-32.97	-88.78	-116.39		9.96	5.56	15.45	9.08	24.51
300.2727	-33.53	-84.72	-124.78		6.08	2.76	7.25	4.29	11.54
301.2700	-33.12	-86.26	-123.80		6.10	2.81	7.51	4.50	12.02
302.2371	-33.40	-81.15	-126.10	-147.99	3.78	2.51	4.16	3.99	8.14
302.3335	-33.83	-82.55	-125.54	-146.35	4.31	2.99	5.00	5.19	10.19
305.3197	-32.60	-80.17	-123.00	-149.13	4.47	2.48	5.28	3.70	8.98
318.3163	-33.33	-87.39	-117.75	-145.76	6.87	2.96	8.52	4.71	13.24
319.2258	-34.53	-85.78	-119.61	-148.84	5.13	2.49	6.17	3.80	9.97
319.2258	-33.78	-85.52	-119.87	-147.90	5.37	2.55	6.61	4.02	10.63
324.2252	-33.81	-84.19	-129.36	-146.43	4.61	1.98	6.12	2.44	8.57
326.2485	-31.67	-88.20	-126.89	-144.20	4.54	2.08	5.82	2.38	8.20
329.2959	-32.59	-90.09	-123.75	-144.31	6.13	2.53	8.18	3.34	11.52
330.2104	-32.66	-93.40	-124.78		6.90	2.84	9.82	4.25	14.08
333.2262	-31.33	-85.96	-129.75	-143.42	5.24	2.11	7.09	2.39	9.48
339.3314	-31.56	-84.86		-143.90	3.97	1.96	4.81	2.33	7.14
347.2058	-32.88	-88.61		-147.81	4.00	2.19	5.08	2.65	7.74
357.3326	-32.73	-87.33		-145.05	2.80	1.73	3.32	1.49	4.81
360.4125	-32.51	-90.11	-127.50	-152.23	4.77	2.66	6.78	3.81	10.59
360.5003	-32.23	-90.61	-126.46	-149.75	5.45	2.71	7.55	4.03	11.58
361.3819	-32.96	-96.03		-147.32	6.02	2.71	8.80	3.99	12.79
361.4455	-32.84	-95.02		-148.05	5.92	2.65	8.48	3.74	12.22
464.1308	-43.36	-104.30	-127.07		16.43	3.59	21.83	5.09	26.93
465.1536	-45.21	-103.18	-127.80		15.45	3.90	23.76	5.44	29.20

Table 3. Results of measurements of parameters of Hβ line.

JD 2458000+	RVkm/s			İnt		EW(Å)		
	R	MU	V	R	V	R	V	R+V
242.3938	-19.55	-71.32	-123.74	3.62	3.00	4.09	2.34	6.43
244.3325	-15.12	-70.91	-123.75	4.19	3.51	5.35	2.93	8.28
263.3932	-32.54	-70.36	-132.60	2.92	2.51	2.66	2.26	4.92
274.3800	-21.58	-71.30	-104.22	2.23	1.63	3.71	0.81	4.52
286.4109	-22.64	-71.71	-113.63	2.77	1.83	2.67	0.98	3.65
289.2479	-29.78	-71.73	-110.65	4.38	3.01	4.13	2.84	6.97
291.2791	-27.89	-72.12	-111.22	3.07	1.82	3.18	0.81	3.99
292.2497	-18.78	-71.59	-113.89	3.06	2.02	3.41	1.18	4.59
293.2864	-21.01	-71.96	-114.92	3.40	2.29	3.57	1.31	4.88
295.3231	-30.46	-72.30	-123.61	3.89	2.81	3.69	2.49	6.18
295.3921	-26.69	-73.39	-125.94	3.84	2.31	3.90	1.41	5.31
296.4028	-31.90	-73.19	-134.80	5.85	4.54	6.40	5.94	12.37
298.4840	-29.78	-74.94	-126.41	8.15	4.08	8.90	5.36	14.26
299.2693	-32.84	-79.45	-109.03	13.19	8.47	12.83	11.12	23.95
299.3352	-31.71	-80.40	-109.87	12.84	8.02	12.78	10.71	23.49
300.2727	-31.31	-75.68	-116.67	6.47	3.36	6.50	4.60	11.09
301.2700	-30.00	-74.96	-111.40	4.88	2.77	4.70	3.19	7.90
302.2371	-25.92	-71.83	-137.74	4.07	3.10	4.39	4.00	8.40
302.3335	-26.53	-72.16	-134.38	4.66	3.99	5.23	6.05	11.28
305.3197	-25.47	-73.36	-132.24	5.67	3.13	6.25	3.89	10.15
318.3163	-30.82	-79.48	-137.88	4.50	2.63	4.57	2.61	7.20
319.2258	-33.68	-78.61	-150.18	3.36	2.20	3.22	1.55	4.78
319.3172	-30.03	-74.87	-149.10	3.19	2.08	2.83	1.20	4.10
324.2252	-23.40	-79.68	-138.03	3.51	1.36	3.90	0.30	4.12
326.2485	-29.26	-80.11	-145.35	3.78	1.57	4.08	0.61	4.69
329.2959	-30.56	-79.54	-114.00	2.55	1.87	4.28	0.86	5.14
330.2104	-28.89	-83.12	-136.33	3.79	1.77	3.62	0.88	4.50
333.2262	-27.21	-79.64	-144.54	4.41	1.48	4.53	0.36	4.89
339.3314	-29.84	-77.49	-153.23	2.58	1.47	2.54	0.51	3.05
347.2058	-12.74	-80.77	-141.11	3.43	2.23	4.03	1.23	5.26
357.3326	-7.38	-81.64	-145.22	3.11	1.86	3.69	1.05	4.74
360.4125	-30.12	-84.25	-147.68	4.65	2.79	5.11	2.02	7.13
360.5003	-29.71	-84.49	-145.58	4.20	2.46	4.52	1.58	6.10
361.3819	-23.09	-85.64	-147.57	3.95	2.69	4.35	1.94	6.29
361.4455	-22.48	-85.92	-147.91	3.81	2.45	4.23	1.52	5.75
464.1308	-54.62	-102.14	-121.35	12.45	6.02	17.54	7.04	24.58
465.1536	-52.36	-100.12	-120.83	12.26	6.13	18.13	6.48	24.61

with strengthening of HeI 5876 line (increasing of the intensity), strong emission lines appear in the red wing of the NaI doublet lines and it converts to P Cyg type of profile. Both of the doublet lines of NaI demonstrate binary structure compris-

ing of deep adsorption especially in the bright period of the star. HeI 5876 line almost disappears in maximum brightness and even large adsorption is observed. In the table 4 the results of spectrophotometric measurements of HeI 5876 and NaI doublet lines have been introduced. Ray speeds of each component of the NaI doublet lines demonstrates very close values. Ray speeds of the R components of D1 and D2 lines are varying in -73 ÷ -85 km/s interval and ray speed of the V component is varying in -97 ÷ -103 km/s interval. R-red component demonstrates the same radial speed with neutral hydrogen zone, i.e., the central absorption of Hydrogen lines (Fig.4). It is assumed that the R obsorption components of lines NaI D1 and D2 arise in the neutral absorption region.

Deepness of R and V components of NaI D1 line change in 0.59÷0.81 and 0.40÷0.86 interval respectively.

7. ANALYSIS OF PARAMETERS OF Hα AND H LINES BY USING THE LIGHT CURVE

V light curve comparison of equivalent width and components' intensity of Hα and Hβ lines in the spectrum of CH Cyg symbiotic star have been introduced in the Fig.5 and 6 respectively. In the figures the right axes are in the increasing order towards to down. Comparison of equivalent widths of Hα and Hβ lines with light curve shows that, the typical feature for symbiotic stars - increase in equivalent width with decrease in brightness - is observed here. This principle failed in Hα line in the dramatic phase (short term change in brightness) of the star.

As it is seen from the picture, character of changes in component's intensity and equivalent width of Hβ line during the observation period fully coincide with changes of brightness in V filter. It makes opposite correlation, it means, equivalent width and intensity of the line increases as the brightness decreases.

8. ANALYSIS OF NAI DOUBLET AND HEI 5876 LINES BY USING THE LIGHT CURVE V

In the Fig.7 it is given the comparison of intensity of R components of NaI doublet lines with V light curve. As it is seen from the picture, changes of intensity of red components of D1 and D2 adsorption lines are the same for both lines and it demonstrates identical character with changes in light curve in V filter. Decrease in the deepness of the line is observed by decrease in brightness.

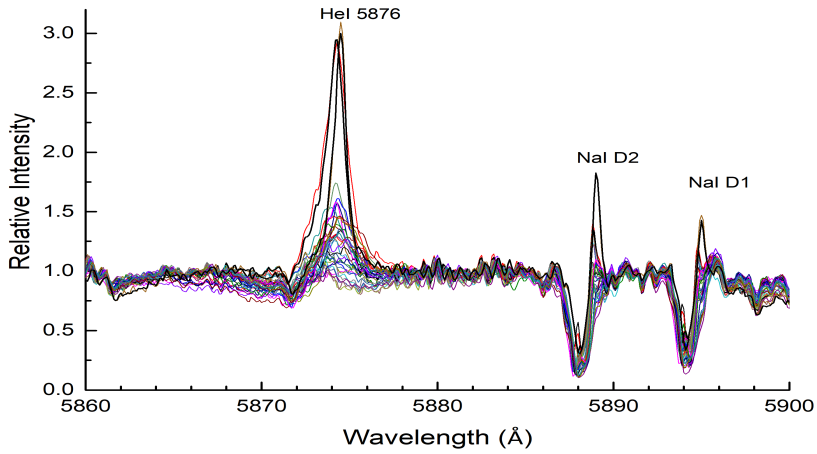

Fig. 3. Profiles of HeI λ 5876 and NaI D1, D2 lines.

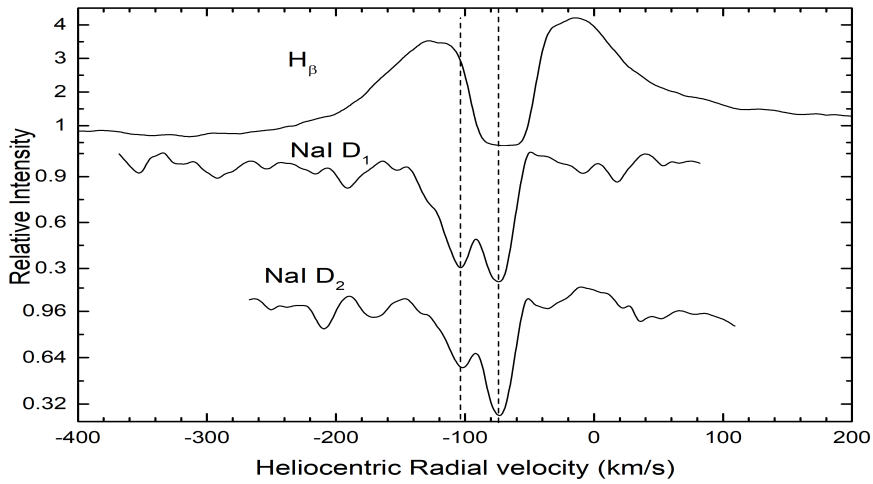

Fig. 4. Profiles of Hβ and NaI D1 and D2 lines.

9. ANALYSIS OF HEI 5876 LINE WITH V LIGHT CURVE.

V light curve comparison of HeI 5876 line intensity and equivalent width has been introduced in the Fig. 8. As it is seen from the figure, convenience is observed in the character of changes of graphs if we do not consider the dramatic phase of the star. Values of equivalent width and intensity increases with decrease in the value of brightness. Usually, line's intensity and equivalent width decreases down

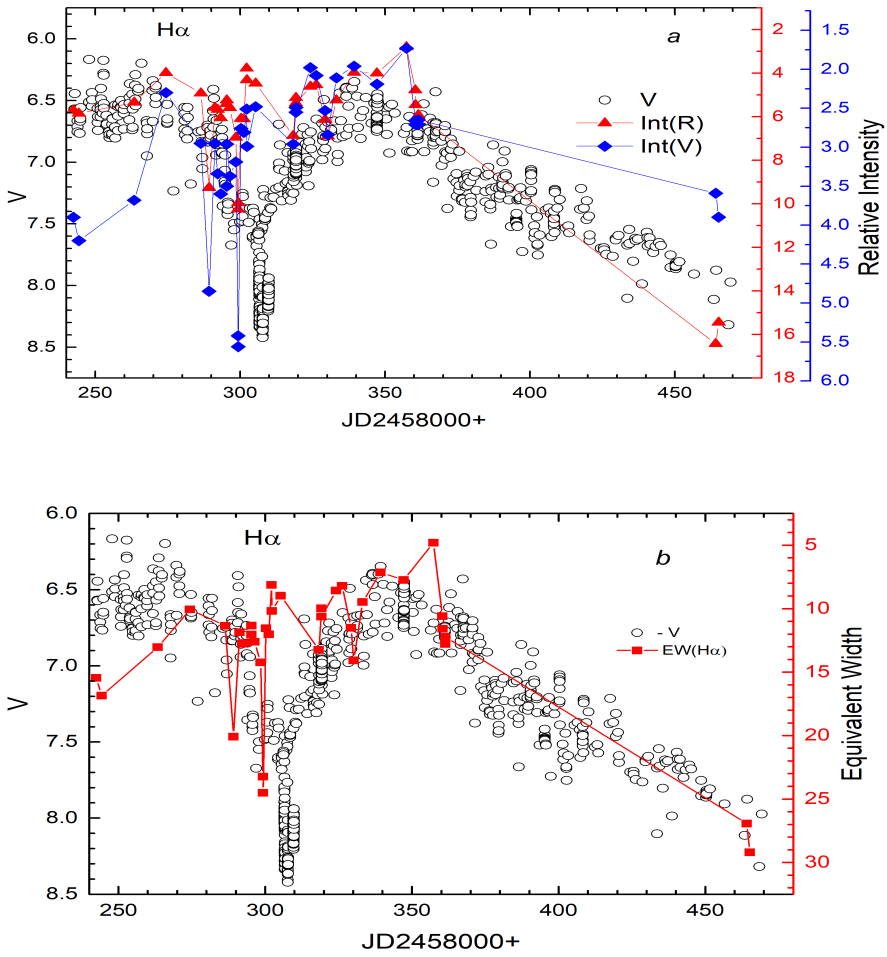

Fig. 5. Time changes of V light curve of CH Cyg symbiotic star and spectrophotometric parameters of Hα line. a – changes in intensities, b – changes in equivalent width, ○ – V filter light curve, ▲- intensity of R component, ♦ - intensity of V component, ■ - equivalent width.

to seamless spectrum level as the brightness increases. Even it was observed that HeI 5876 line disappeared for 3 days in the maximum of brightness.

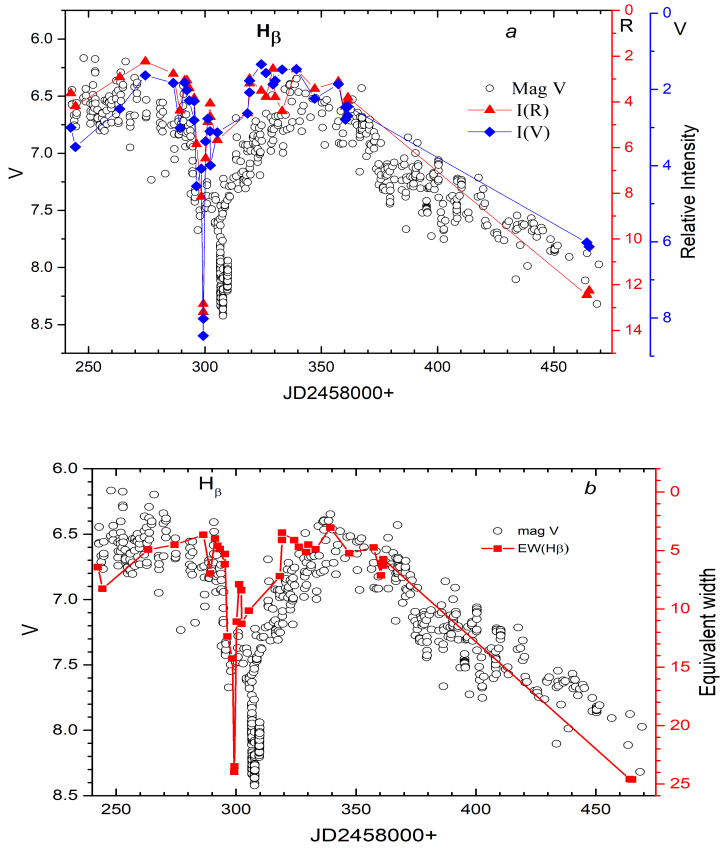

Fig. 6. Time changes of V light curve of CH Cyg symbiotic star and spectrophotometric parameters of Hβ line. a – changes in intensities, b – changes in equivalent width, ○ – V filter light curve, ▲- intensity of R component, ♦ - intensity of V component, ■ - equivalent width.

10. ANALYSIS OF CHANGES IN CH CYG SYMBIOTIC STAR

In some of our spectra V component of the Hα and Hβ lines and HeI 5876 line was found with complex structure and multiple components. As we already know, the emission lines are formed in the cloud around the hot star and enlargement of the surrounding cloud can lead to formation of several components. Existence of adsorbing substance around the star in the visual direction causes formation of the central adsorption in the profile of the emission lines. In most cases central adsorption gets a very close speed to the mass center speed (-60 km/s). But if we don't consider the spectra achieved in the last two dates of our observation, the central adsorption slides towards the blue side of the spectrum

Table 4. Results of measurements of NaI doublet and HeI 5876 lines.

JD 2458000+	NaI D1					NaI D2						HeI 5876	
	RV		Int		EW	RV		Int		EW		Int	
	R	V	R	V	R+V	R	V	R	V	R+V			
242.3938	-73.2	-102.3	0.76	0.40	0.59	-74.6	-103.7	0.79	0.64	0.83	-48.8	1.33	0.59
244.3325	-73.8	-101.8	0.74	0.41	0.59	-75.4	-103.9	0.78	0.69	0.84	-62.5	1.46	1.26
263.3932	-73.1	-102.4	0.78	0.67	0.99	-75.4	-103.7	0.81	0.84	1.29	-111.6	1.15	0.26
274.3800	-76.9	-102.9	0.81	0.80	0.92	-79.3	-105.3	0.82	0.89	1.12			
286.4109	-74.7	-102.9	0.79	0.61	0.88	-77.1	-104.2	0.81	0.80	1.13	-71.4	1.11	0.14
289.2479	-74.5	-99.3	0.78	0.57	0.81	-76.6	-103.2	0.80	0.79	1.03	-59.9	1.56	0.62
291.2791	-75.3	-100.8	0.79	0.61	0.81	-77.5	-103.8	0.80	0.79	1.04	-38.1	1.10	0.18
292.2497	-74.3	-102.1	0.80	0.64	0.95	-90.4	-103.9	0.81	0.81	1.30	-65.6	1.29	0.87
293.2864	-75.1	-102.3	0.77	0.66	0.98	-78.4	-104.6	0.78	0.86	1.28	-65.4	1.37	0.75
295.3231	-75.8	-102.8	0.74	0.70	0.84	-78.7	-104.8	0.76	0.85	1.07	-84.0	1.07	0.07
295.3921	-77.0	-102.5	0.73	0.70	0.83	-80.6	-104.7	0.74	0.85	1.09	-88.5	1.12	0.11
296.4028	-79.0	-102.2	0.67	0.71	0.73	-84.3	-104.0	0.72	0.84	0.92	-84.0	1.53	1.00
298.4840	-73.4	-101.0	0.65	0.71	0.70	-82.4	-103.4	0.68	0.81	0.85		1.32	0.60
299.2693	-77.8	-101.8	0.59	0.67	0.65	-82.0	-104.3	0.65	0.82	0.82		2.90	3.39
299.3352	-77.1	-101.3	0.59	0.68	0.65	-82.0	-103.7	0.64	0.80	0.81	-64.6	2.95	2.74
300.2727	-81.3	-102.4	0.64	0.68	0.68	-84.2	-105.2	0.67	0.79	0.85	-100.2	1.10	0.06
301.2700	-79.0	-101.6	0.65	0.72	0.72	-83.7	-104.7	0.71	0.84	0.93		1.04	0.02
302.2371	-82.4	-99.7	0.69	0.75	0.82	-87.4	-104.5	0.74	0.81	0.97		1.07	0.01
302.3335	-81.5	-101.6	0.66	0.75	0.76	-86.0	-105.4	0.71	0.79	0.92	-97.6	1.22	0.24
305.3197	-83.8	-98.5	0.67	0.77	0.72	-86.9	-101.8	0.73	0.82	0.89			
318.3163	-77.7	-100.5	0.74	0.75	0.87	-82.0	-102.8	0.79	0.86	1.07	-68.2	1.74	1.29
319.2258	-80.3	-100.9	0.78	0.78	0.91	-84.8	-102.5	0.81	0.88	1.12	-81.7	1.25	0.37
319.2258	-80.6	-101.1	0.77	0.79	0.92	-85.0	-103.4	0.82	0.88	1.15	-82.9	1.15	0.16
324.2252	-79.6	-101.1	0.77	0.79	0.89	-86.4	-102.8	0.81	0.87	1.12	-61.5	1.20	0.33
326.2485	-79.7	-101.0	0.74	0.70	0.80	-80.9	-103.3	0.76	0.84	1.02	-71.3	1.30	0.63
329.2959	-78.2	-102.1	0.72	0.68	0.79	-82.4	-101.7	0.78	0.83	1.08	-64.4	1.60	0.97
330.2104	-76.0	-100.9	0.70	0.63	0.76	-78.6	-102.9	0.77	0.82	1.06	-70.6	1.57	0.72
333.2262	-78.0	-99.8	0.74	0.68	0.83	-81.1	-103.1	0.80	0.82	1.04	-72.3	1.39	0.80
339.3314	-77.9	-98.4	0.79	0.75	0.98	-84.5	-100.7	0.85	0.89	1.21	-56.2	1.10	0.11
347.2058	-82.5	-98.4	0.78	0.80	1.05	-83.4	-99.8	0.82	0.88	1.28	-59.8	1.26	0.51
357.3326		-97.2		0.86	1.14		-101.5		0.90	1.37			
360.4125		-99.8		0.82	1.05		-102.7		0.88	1.21	-44.9	1.46	1.05
360.5003		-99.4		0.82	1.06		-101.8		0.89	1.26	-55.1	1.45	0.93
361.3819	-81.9	-99.9	0.72	0.78	0.99	-84.5	-101.4	0.78	0.87	1.10	-62.7	1.35	0.61
361.4455	-83.5	-99.4	0.73	0.79	1.00	-86.4	-102.0	0.80	0.88	1.14	-70.8	1.32	0.56
464.1308		-101.1		0.68	0.50		-105.3		0.76	0.63	-65.5	3.07	2.07
465.1536		-100.4		0.66	0.51		-104.5		0.69	0.60	-66.0	2.95	2.16

in about 20 -25 km/s and demonstrates the speed of $\sim$ -70 km/s, -85 km/s. This is because the speed of the wind of the adsorbing particles in the neutral hydrogen region is greater than the speed of wind of released particles in the ionized

region. Absorption particles arrive in sooner than released particles. Deepness of the adsorbing component shows the density of the star wind (Burmeister M., and Leedjarv L.,2007). Also, if we consider that, Hα and Hβ lines form in the disc around the star, formation of binary component profile can be explained by this factor. Rapid destruction of binary component profile and especially decreasing the intensity of V component are explained by destruction of the disc (Burmeister, M. and Leedjarv, L., 2007). V/R proportion's being always less than 1 in our observations shows that continuous substance fow exists from the hot star.

Short term rapid changes in the star can be explained with the fact that, being in proximity for some years gives its effect when the hot star of the symbiotic system gets closer to the giant star, i. e., when the star moves through the periastron (Because the period is very long in CH Cyg star - 15 years). In this period intensity and amount of fow of substance from the giant star increases. As a result of that, stability of the disc around the hot star spoils and jet of substances are observed from the hot star and this is followed by rapid changes in Hα and Hβ lines (Wallerstein et al. 2010).

Emission lines with high ionization potential, including HeI 5876 are formed in the region near the hot star. Rapid changes in the HeI 5876, getting disappeared of the line and formation can be related to changes of ultraviolet rays emitting from the hot star. Photometric rapid changes prove that firmly.

The fact of ray speeds of NaI D1 and D2 doublet lines red components and central adsorption of Hα and Hβ getting the same value confirms that they have been formed in the same environment and in the neutral region around the star.

Increase in the deepness of red component of D1 and D2 lines of NaI with increase of brightness of the star can be estimated a result of enrichment of the neutral region with Na atoms and vice versa. The other approach is also possible. Decrease in the brightness of the star after the active phase of the symbiotic star CH Cyg can be explained with screening too. Strong release of substance in the active period results in getting the gas-dust cloud denser around the star. As a result of that, the star becomes screened and brightness decreases. Formation of a strong emission in the red wing of the NaI doublet lines and at the same time reinforcement of the emission lines λ6548 Å and λ6584 Å of [NII] which is the main indicator of the gas-dust cloud once again proves that. The same time increase in the equivalent width and intensity of Hα, Hβ and HeI 5876 lines in several times while rapid collapse decreasing of brightness can be explained with changes in the density of the surrounding cover.

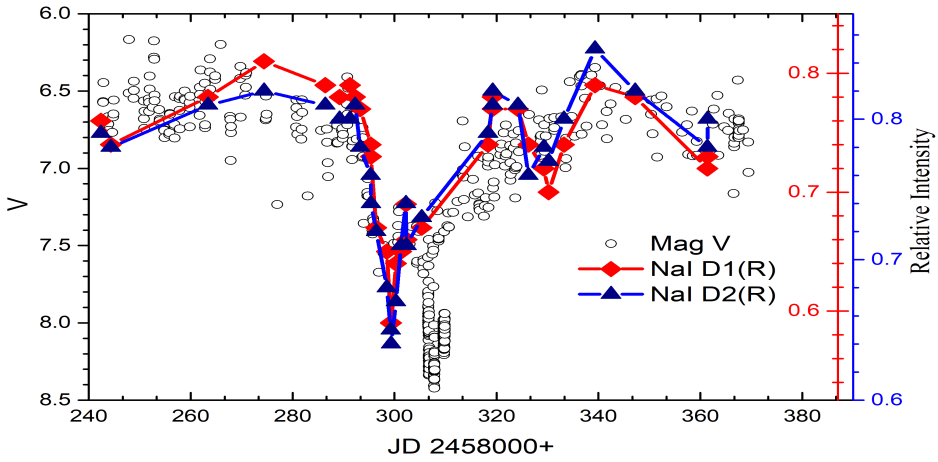

Fig. 7. Timely changes of V light curve of CHCyg symbiotic star and deepness of red components of NaI doublet lines of D1 and D2. ○ – V filter light curve,♦ and ▲ -deepness of D1 and D2 lines respectively.

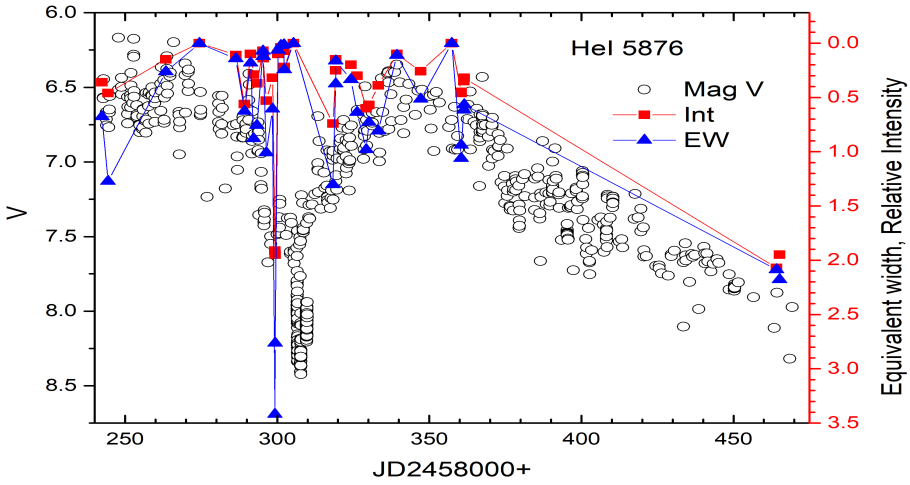

Fig. 8. Time based change of intensity and equivalent width of HeI 5876 and V filter light curve of CH Cyg symbiotic star. ○ – brightness in the V filter, ■–intensity, ▲–equivalent width.

11. THE MAIN RESULTS

Following results have been summarized from the analysis of the CCD echelle spectra of CH Cyg symbiotic system achieved in 2018 for the first time.

1. Spectrophotometric parameters of Hβ emission line such as equivalent width, intensity of the red and violet components provide alteration with the same character and opposite phase changes with light curve in V filter.

2. Profiles of both D1 and D2 doublet lines of NaI represents binary component structure and changes in the intensity of both lines' red component match with the character of changes in V light curve.

3. Rapid alteration of HeI λ 5876 Åline and full disappearing of emission have been observed.

4. Absorption jets with the speed of -800km/s have been observed in the violet wing of Hβ and HeI λ 5876 lines.

REFERENCES

1. Abdullayev, B.I., Alekberov, I.A., Gulmaliyev, N.I,.et al., 2012, Azerbaijani Astronomical Journal, №4, p.39-47.

2. Burmeister, M.; Leedjärv, L., 2009, Astronomy and Astrophysics, v. 504, Issue 1, 2009, pp.171-180.

3. Contini, M., Angeloni, R., Rafanelli, P., 2009, Astronomische Nachrichten, Vol.330, Issue 8, p.816.

4. Deutsch, A.J., 1964, Ann. Rep. Mt. Wilson and Palomar Obs.1963-1964, p.11-15.

5. Gaposchkin, S., 1952, The Observatory, vol.118, p.155-163.

6. Hinkle, K. H., Fekel, F.C., Johnson, D.S., Scharlach W.W.G., 1993, AJ, 105,107.

7. Hinkle K.H., Fekel F.C., Joyce R., 2009, ApJ, 2009, 692, 1360.

8. Iijima, T., Naito, H. and Narusawa, S., 2018, Astronomy & Astrophysics, v.622, A45, p.2-15.

9. Joy, Alfred H., 1942, ApJ, 96, 344.

10. Mikailov, Kh. M.; Khalilov, V. M., 2005, Kinematika i Fizika Nebesnykh Tel, vol. 21, no. 6, p. 452-460.

11. Mikailov, Kh. M.; Musaev, F. A.; Alekberov, I. A.; Rustamov, B. N.; Khalilov, O. V., 2020, Kinematics and Physics of Celestial Bodies, 2020, vol. 36, issue 1, pp. 22-36.

12. Mikolajewski, M., Mikolajewska, J., Khudiakova, T. N., 1990, Astronomy and Astrophysics, vol. 235, no. 1-2, p. 219-23.

13. Mikołajewski, M., Mikołajewska, J., Tomov, T., Kulesza, B., Szczerba, R., 1990, AcA, 40, 129.

14. Skopal, A, Vanko, M., Pribulla, T., et al., 1996, Mon. Not. Roy. Astron. Soc. 282, 327.

15. Van Leeuwen, F., 2007, Astrophysics and Space Science Library, Volume 350.

16. Wallerstein, George; Munari, U.; Siviero, A.; Dallaporta, S.; Dalmeri, I., 2010, Publications of the Astronomical Society of the Pacific, V. 122, Issue 887, pp. 12-16. www.gazinur.com/DECH-software.htm https://www.aavso.org/lcg